Visual Neuroscience (1992), **8**, 365–372. Printed in the USA.

Temporal-frequency tuning of direction selectivity in cat visual cortex

ALAN B. SAUL AND ALLEN L. HUMPHREY

Department of Neurobiology, Anatomy, and Cell Science, University of Pittsburgh School of Medicine, Pittsburgh

(RECEIVED June 25, 1991; ACCEPTED September 16, 1991)

Abstract

Responses of 71 cells in areas 17 and 18 of the cat visual cortex were recorded extracellularly while stimulating with gratings drifting in each direction across the receptive field at a series of temporal frequencies. Direction selectivity was most prominent at temporal frequencies of 1–2 Hz. In about 20% of the total population, the response in the nonpreferred direction increased at temporal frequencies of around 4 Hz and direction selectivity was diminished or lost. In a few cells the preferred direction reversed.

One consequence of this behavior was a tendency for the preferred direction to have lower optimal temporal frequencies than the nonpreferred direction. Across the population, the preferred direction was tuned almost an octave lower. In spite of this, temporal resolution was similar in the two directions. It appeared that responses in the nonpreferred direction were suppressed at low frequencies, then recovered at higher frequencies.

This phenomenon might reflect the convergence in visual cortex of lagged and nonlagged inputs from the lateral geniculate nucleus. These afferents fire about a quarter-cycle apart (i.e. are in temporal quadrature) at low temporal frequencies, but their phase difference increases to a half-cycle by about 4 Hz. Such timing differences could underlie the prevalence of direction-selective cortical responses at 1 and 2 Hz and the loss of direction selectivity in many cells by 4 or 8 Hz.

Keywords: Temporal frequency, Direction selectivity, Visual cortex, Lateral geniculate nucleus, Lagged cells

Introduction

The origins of direction selectivity in the visual cortex remain unclear despite intensive study. Multiple mechanisms may underlie both long-range (Eysel et al., 1987, 1988) and short-range processes (Barlow & Levick, 1965; Emerson & Gerstein, 1977; Baker & Cynader, 1986). Explanations of short-range direction selectivity have recently focused on spatiotemporal quadrature models (Watson & Ahumada, 1983, 1985; Adelson & Bergen, 1985; Van Santen & Sperling, 1985; Shadlen & Carney, 1986), in which bidirectional inputs that are out of phase with each other by a quarter-cycle in space and in time combine to create unidirectional outputs. This broad class of models leaves open the identification of the model elements with neural structures. The spatial separation between the inputs presumably arises from spatial receptive-field differences, which are ubiquitous. The substrate for temporal differences is less obvious. Delays ranging from 25–250 ms are needed to cover a temporal-frequency range of 10–1 Hz. Intracortical mechanisms producing such timing changes have yet to be described.

Responses that are in temporal quadrature have recently been described in the lateral geniculate nucleus (LGN), however. X- and Y-relay cells in the A layers of the cat LGN can be classified as lagged or nonlagged (Mastronarde, 1987; Humphrey & Weller, 1988*a*; Mastronarde et al., 1991), and this distinction is largely related to response timing (Saul & Humphrey, 1990*a*). Lagged and nonlagged cells fire about a quarter-cycle apart at low temporal frequencies. We showed that simulating the convergence of *average* lagged and nonlagged inputs onto a hypothetical cortical cell led to direction selectivity (Saul & Humphrey, 1989, 1990*a*). These simulations also led to several predictions about the properties of the cortical direction selectivity. First, because the average lagged and nonlagged cells are in temporal quadrature only at low temporal frequencies, a simulation based on such inputs produced direction-selective outputs only at low temporal frequencies. The model cortical cell lost direction selectivity at about 4 Hz. Second, reversal of the preferred direction was seen beyond 4 Hz as the phase difference between the inputs reached a half-cycle. Third, dramatic reversals were avoided because the average lagged response was much weaker than the average nonlagged response at high temporal frequencies. Above about 4 Hz the simulated cortical cell responded like its nonlagged input. In particular, the cell was not direction selective at high temporal frequencies. We also showed that simulating the convergence of individual lagged and nonlagged cells could lead to more robust direction selectivity (Fig. 14C in Saul & Humphrey, 1990*a*).

In reviewing the literature on cortical direction selectivity, we

Reprint requests to: Alan B. Saul, Department of Neurobiology, Anatomy, and Cell Science, University of Pittsburgh School of Medicine, Pittsburgh, PA 15261, USA.

found that there was little or no information on the relation between temporal frequency and direction selectivity. Most studies have examined direction selectivity as a function of the speed of a moving slit or bar (Goodwin & Henry, 1978; Orban et al., 1981; Duysens et al., 1987). A few studies have tested direction selectivity over a range of temporal frequencies. Holub and Morton-Gibson (1981) reported different tuning curves for opposite directions of motion, and Reid (1988) showed declining direction selectivity with temporal frequency. However, we are unaware of any previous study that has documented the temporal-frequency dependence of direction selectivity in any detail. Given the clear predictions of our model, we performed a simple single-unit recording experiment in cat primary visual cortex, measuring temporal-frequency tuning in opposite directions of motion. We found that direction selectivity in many cells varies with temporal frequency in a manner consistent with their receiving inputs from lagged and nonlagged neurons. Some of these results have been briefly presented in abstracts (Saul & Humphrey, 1990*b*, 1991).

Methods

Cats were prepared for single-unit recording from the visual cortex much as described previously for LGN recordings (Saul & Humphrey, 1990*a*), with the exception that anesthesia was maintained during surgery using 1–1.5% halothane in nitrous oxide and oxygen (70:30), and during recording using 0.1–0.5% halothane in the N_2O/O_2 gas mixture. No barbiturates were used during or prior to recording in any of these experiments. Heart rate, expired CO_2, and the cortical electroencephalogram were monitored throughout the experiment. Single neurons were recorded extracellularly using glass micropipettes filled with 10% HRP (Sigma, St. Louis, MO) in 0.2 M KCl and Tris buffer. We used these high-impedance electrodes (50–100 MΩ) in order to sample neurons with small as well as large somata (Mullikin et al., 1984; Humphrey & Weller, 1988*b*).

For each cell, the optimal orientation and minimal response field of the dominant eye were determined by hand plotting. Receptive-field structure was quantitatively determined from line-weighting functions generated by bar stimuli presented on a Tektronix 608 monitor placed 57 cm from the eye. Spatial-frequency tuning curves in each direction were obtained using sinusoidal gratings drifting at the optimal orientation at the estimated optimal temporal frequency (usually 2 or 4 Hz). For the present study, the stimulus protocol consisted of sinusoidal gratings at the preferred orientation and spatial frequency drifting in each direction at several temporal frequencies. Gratings were masked for strongly end-stopped cells. Contrasts were either 40 or 50% about a mean luminance of 25 cd/m^2.

Responses were compiled into histograms representing the average firing rate during each stimulus cycle for each trial. Stimulus trials were generally 4 s long, although in a few cases 10-s or 16-s trials were used in order to accommodate testing at low temporal frequencies (trial length was always constant during a single run, however). Means and standard errors over the 5–10 trials for each stimulus condition were computed, using both the d.c. (for complex cells) and first harmonic (for simple cells) components of the response. Simple and complex cells were distinguished based on the segregation of ON and OFF zones in hand plots and in the quantitatively obtained line-weighting functions, as well as larger first harmonic than d.c. response amplitudes when tested with drifting gratings (De Valois et al., 1982).

The preferred direction was chosen to be that giving the greater response averaged over all of the temporal frequencies tested (except in one case noted below). As an index of direction selectivity, for each temporal frequency the two directions were compared using the *t*-statistic between them (i.e. the difference of the means divided by the square root of the summed squared standard errors). This provided a more consistent normalization than arithmetic indices such as the difference of the responses in each direction divided by their sum. Our criterion for direction selectivity was a *t*-score exceeding 2.

A difference-of-Gaussians function was fit to the response amplitude *vs.* temporal-frequency tuning curves for each direction, using a Levenberg-Marquardt method (Press et al., 1986). This function was chosen simply because it provided good fits to the data, with no underlying mechanisms implied. The data were weighted by the reciprocals of the standard errors and the square roots of the response amplitudes. Parameters were reinitialized several times to help ensure valid fits. Some nonpreferred direction tuning curves could not be fit (generally indicated by a singular covariance matrix in the fitting algorithm) because responses were too weak. The four parameters of the difference-of-Gaussians function (amplitudes and half-widths for the two Gaussians) were used to derive values for optimal temporal frequency, temporal resolution (frequency above the optimum giving 10% of the peak response), and width of the tuning curve at half-height. For some fits, tuning width was undefined because the curve never reached half-height on the low-frequency end. We rejected values of temporal resolution above 70 Hz as spurious, although only one such case was encountered, all other values being under 40 Hz.

We marked the end of a penetration by ejecting horseradish peroxidase (HRP). At the end of the experiment, the animal was killed with an intravenous injection of nembutal and perfused transcardially with 1% paraformaldehyde and 2% glutaraldehyde. The brain was blocked in the plane of the penetrations, cut at 50 or 100 μm, reacted to reveal the HRP, and counterstained with cresyl violet. Electrode tracks were reconstructed and laminar positions of recording sites were estimated using criteria described in Humphrey et al. (1985).

Results

Data were obtained from 57 cells (44 simple, 13 complex) in area 17 and 14 cells (9 simple, 5 complex) in area 18. The main results were similar in areas 17 and 18, and across simple and complex cells, so that data were pooled in some cases. Most cells (51 of 71, 72%) responded sufficiently even in their nonpreferred directions to permit estimation of tuning parameters.

This report focuses on the phenomenon illustrated in Fig. 1A. Temporal-frequency tuning curves from an area 17 simple cell are shown for each direction of motion. The nonpreferred direction (dashed line) produced almost no response at low frequencies, up to 1 Hz, even though responses were vigorous in the preferred direction. At 4 Hz, the two directions responded equally well. Beyond 4 Hz, the previously nonpreferred direction provided slightly better responses than the previously preferred direction, suggestive of a reversal. However, responses were similar in the two directions at high frequencies.

These effects were not due to spontaneous variability in cortical responsiveness. For example, the behavior of this cell was stable throughout the 7 h during which it was tested repeatedly. Temporal tuning curves were obtained four separate times and always showed an increase in the nonpreferred direction re-

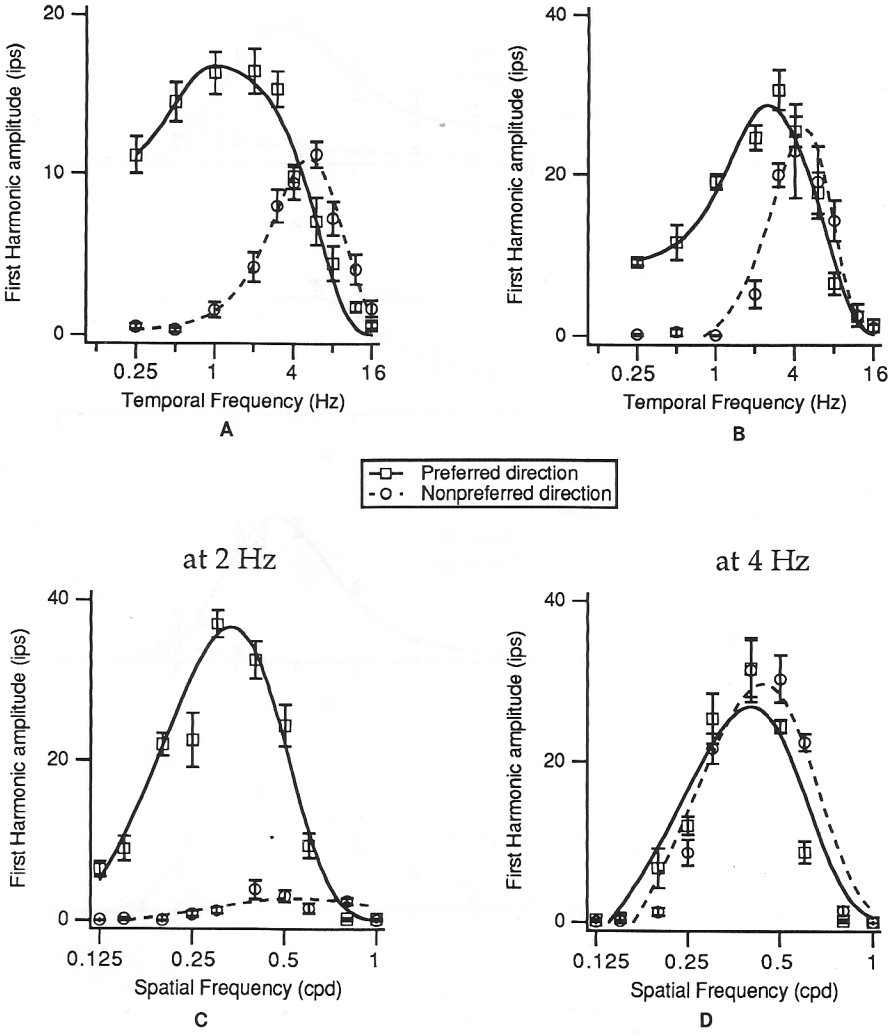

Fig. 1. Tuning curves from an area 17 simple cell recorded in layer 5. In this and the following figures, the square symbols represent average response amplitudes in the preferred direction, and the circles show the nonpreferred direction responses. Error bars represent standard errors. The lines show the best-fitting difference-of-Gaussians functions, the solid curve for the preferred, and the dashed curve for the nonpreferred direction. A: Temporal-frequency tuning curves obtained at 0.2 cpd. B: Temporal-frequency tuning curves obtained at 0.25 cpd about 3 h earlier than those shown in A. C: Spatial-frequency tuning curves obtained at 2 Hz. D: Spatial-frequency tuning curves obtained at 4 Hz.

sponse at high temporal frequencies, with a consequent loss of direction selectivity. Data from one of these other runs are shown in Fig. 1B. Overall response amplitudes varied by about a factor of two (note change of scale), but the characteristic tuning remained. Spatial-frequency tuning curves were obtained at 2 and at 4 Hz, with the former (Fig. 1C) showing strong direction selectivity and the latter (Fig. 1D) almost no direction selectivity.

The phenomenon illustrated in Fig. 1, where cells are direction selective at low temporal frequencies, but lose their direction selectivity at higher frequencies, was observed in many cells to varying degrees. Figure 2 presents ten examples, including both simple and complex cells, and cells from areas 17 and 18. Note that in all of these examples direction selectivity is present at 1 Hz. The nonpreferred direction is often silenced at this point, but begins to respond by 2 or 4 Hz. In cases such as Fig. 2A–2D, both directions yield similar responses at higher frequencies. In Fig. 2E, by 4 Hz the preferred direction response has declined greatly but the two directions give similar responses that differ slightly from zero. The cells illustrated in Figs. 2F–2J retain their direction selectivity up to nearly their resolution limits, but the nonpreferred direction response grows as temporal frequency exceeds about 2 Hz. Although the nonpreferred direction response remains weak in these cells, the small responses around 4 Hz help to reveal the total suppression of activity around 1 Hz. For the simple cells, the reliability of these low response amplitudes was additionally confirmed by the consistency of their response phase values.

The type of tuning illustrated in Fig. 2, which was evident in about 20% of the sample, contrasts with several other behaviors observed. Examples of these contrasting forms of tuning are shown in Fig. 3. About 30% of the cells showed purely direction-selective responses independent of temporal frequency, such as the cell in Fig. 3A. The nonpreferred direction either failed to respond at any frequency in these cells or responded only very weakly across all frequencies. Another 20% of our sample responded to both directions but clearly preferred one direction, and the tuning in each direction was similar (Fig. 3B). About 15% were not direction selective, responding similarly to each direction at all frequencies (Fig. 3C). Several cells, perhaps 7% of the population, reversed their preferred direction, so that one direction was optimal up to 1–4 Hz, then the other direction was preferred up to 8–16 Hz (Fig. 3D). Some of the cells illustrated in Fig. 2 might be put into this category, but were not significantly direction selective at high frequencies. Some cells could not be placed easily into one of the above informal qualitative categories.

To quantify the results across our entire sample, we measured a number of parameters for each cell. One feature evident in Fig. 2 is the lower optimal temporal frequency for the

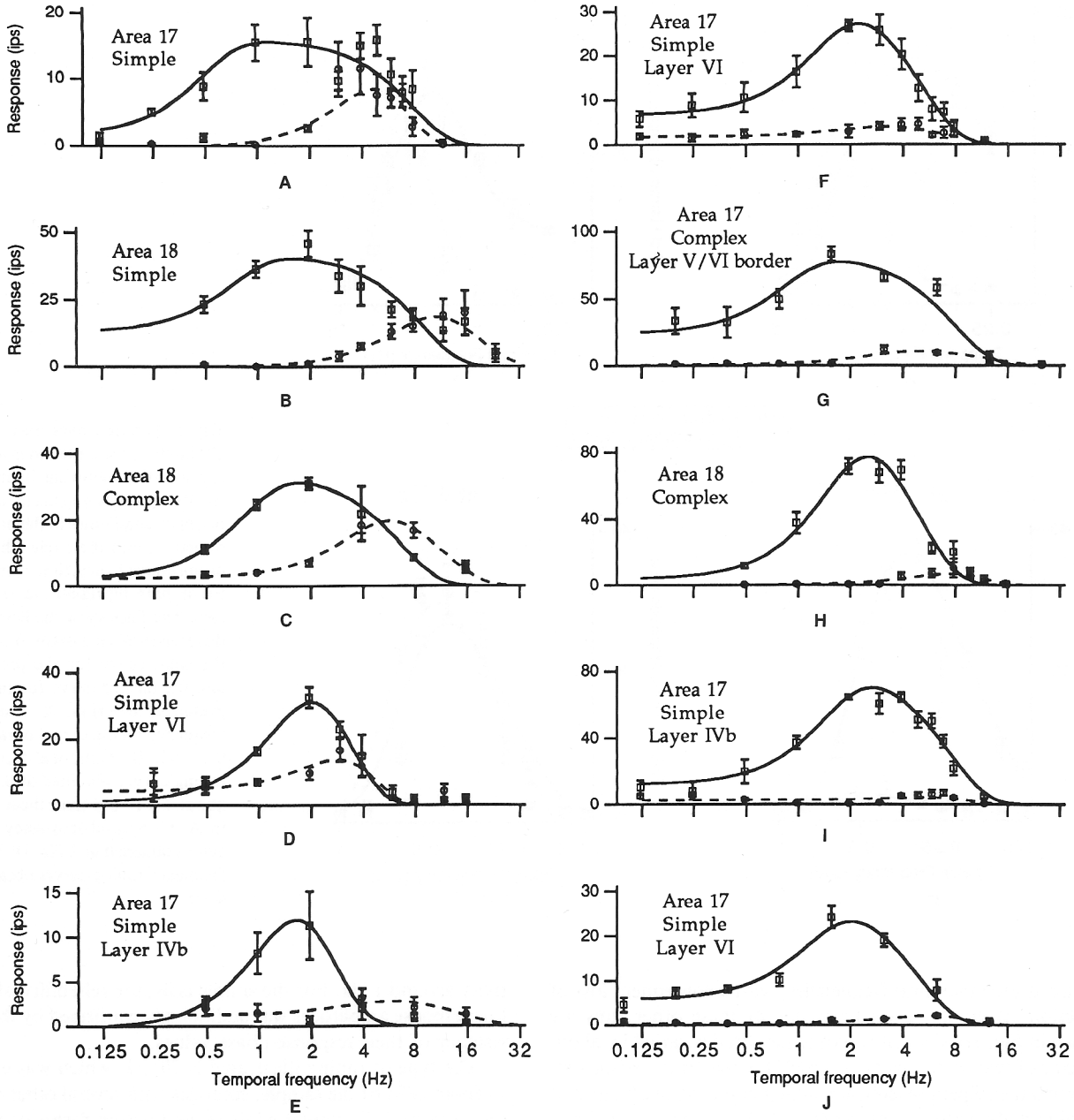

Fig. 2. Ten examples of temporal-frequency tuning curves from cells showing direction selectivity predominantly at low frequencies. Response amplitudes are derived from first harmonics for simple cells and from means for complex cells. Cortical area (17 or 18), cell class (simple or complex), and laminar position are indicated. Laminar position is unknown for the cells in A–C and H. The horizontal axes of all graphs share the same scale, shown in E and J.

preferred direction compared to the nonpreferred direction. In Fig. 4A, we illustrate this comparison, plotting preferred *vs.* nonpreferred direction optimal temporal frequencies. The diagonal line separates cells in which the preferred direction had higher (above the line) or lower (below the line) optimal frequency than the nonpreferred direction. Most of the points fall below the line, illustrating that the response in the nonpreferred direction peaks at relatively high temporal frequencies. Overall, optimal frequencies ranged from 0.4–9 Hz for the preferred direction and from 0.3–13 Hz for the nonpreferred direction, with arithmetic means and standard errors of 3.0 ± 0.2 Hz and 4.9 ± 0.4 Hz, respectively. In the population, therefore, the preferred direction was tuned to significantly lower temporal frequencies ($P < 0.0001$, paired t-test). Table 1 gives mean values for each cell type and cortical area. The largest differences between the directions were found in area 18, where both simple and complex cells had optimal frequencies an octave lower in the preferred direction. Complex cells had slightly higher optimal frequencies, but in no case was this significant at the 0.01 level. For the preferred direction, optimal temporal frequencies were not significantly higher in area 18 than in area 17, despite the larger average eccentricity of our area 18 sample. For the

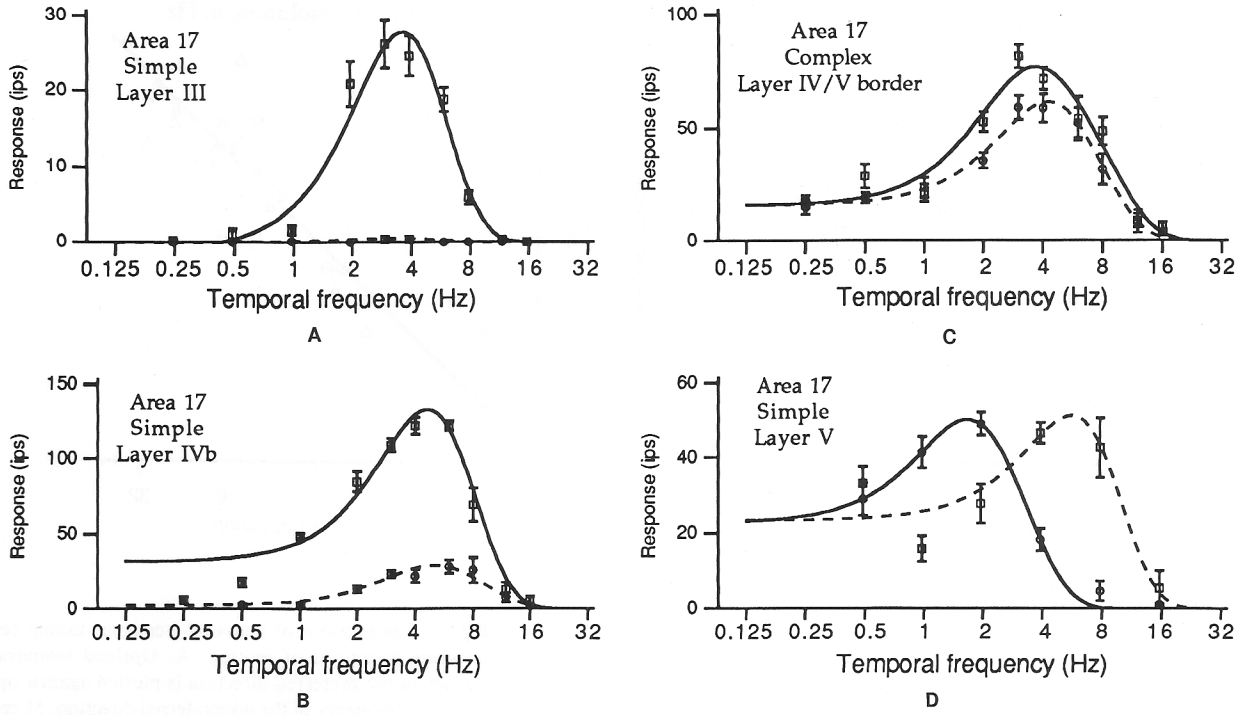

Fig. 3. Four examples of behaviors different from that shown in Figs. 1 and 2. A: Purely direction-selective cell. B: Direction-biased cell. C: Nondirection-selective cell. D: Direction-preference reversing cell. For this last cell, we chose to make an exception to our rule for assigning preferred and nonpreferred labels to the two directions of motion. We took the direction having the lower optimal temporal frequency as the preferred direction. This cell was the only such exception.

nonpreferred direction, tuning was significantly higher in area 18 than in area 17 ($t = 2.9$, $P = 0.005$).

The nonpreferred direction has a higher optimal temporal frequency in these cells not because the whole tuning curve is shifted to the right, but because the response seems to be suppressed at low frequencies. One way to illustrate this point is to compare temporal resolutions, as in Fig. 4B. Again, the line separates regions where the preferred direction has a higher or lower resolution than the nonpreferred direction. Most of the points are close to the line in this case, showing that temporal resolution is similar in the two directions. A few cells fall well below the line, meaning that the nonpreferred direction had higher resolution than the preferred direction. These were the cells in which the preferred direction reversed. Temporal resolution in our sample ranged from 2.1–38 Hz, with means of 14 ± 1 Hz in the preferred direction and 16 ± 1 Hz in the nonpreferred direction. None of the relevant differences shown in Table 1 is significant at the 0.01 level, but the resolution in the preferred direction is uniformly lower.

These results are summarized in Fig. 4C, where the distance

Table 1. *Temporal tuning parameters*[a]

	Eccentricity (deg)	Preferred optimal TF (Hz)	Nonpreferred optimal TF (Hz)	Preferred resolution (Hz)	Nonpreferred resolution (Hz)	Preferred width (octaves)	Nonpreferred width (octaves)
Area 17	5.3 ± 0.3 (54)	2.9 ± 0.3 (57)	4.5 ± 0.4 (42)	13.5 ± 1.0 (57)	15.5 ± 1.2 (41)	3.3 ± 0.2 (50)	3.1 ± 0.1 (35)
Area 18	13.7 ± 1.3 (14)	3.2 ± 0.6 (14)	7.3 ± 0.6 (9)	14.8 ± 1.3 (14)	21.0 ± 2.3 (9)	3.4 ± 0.3 (12)	2.7 ± 0.1 (8)
Simple	6.7 ± 0.6 (51)	2.8 ± 0.3 (53)	4.9 ± 0.5 (37)	12.9 ± 0.9 (53)	15.5 ± 1.2 (36)	3.3 ± 0.2 (46)	3.0 ± 0.1 (32)
Complex	8.0 ± 1.2 (17)	3.4 ± 0.5 (18)	5.3 ± 0.8 (14)	16.2 ± 2.1 (18)	19.0 ± 2.3 (14)	3.4 ± 0.3 (16)	3.2 ± 0.2 (11)

[a]Numbers are means ± standard errors with sample sizes in parentheses. Nonpreferred direction fits could not be obtained in some cases because responses were too weak. The nonpreferred direction fit for one cell gave temporal resolution of 95 Hz, a spurious value that was rejected. Tuning widths could not be estimated in several cases because the low-frequency tail of the fitted curve did not descend below the half-height.

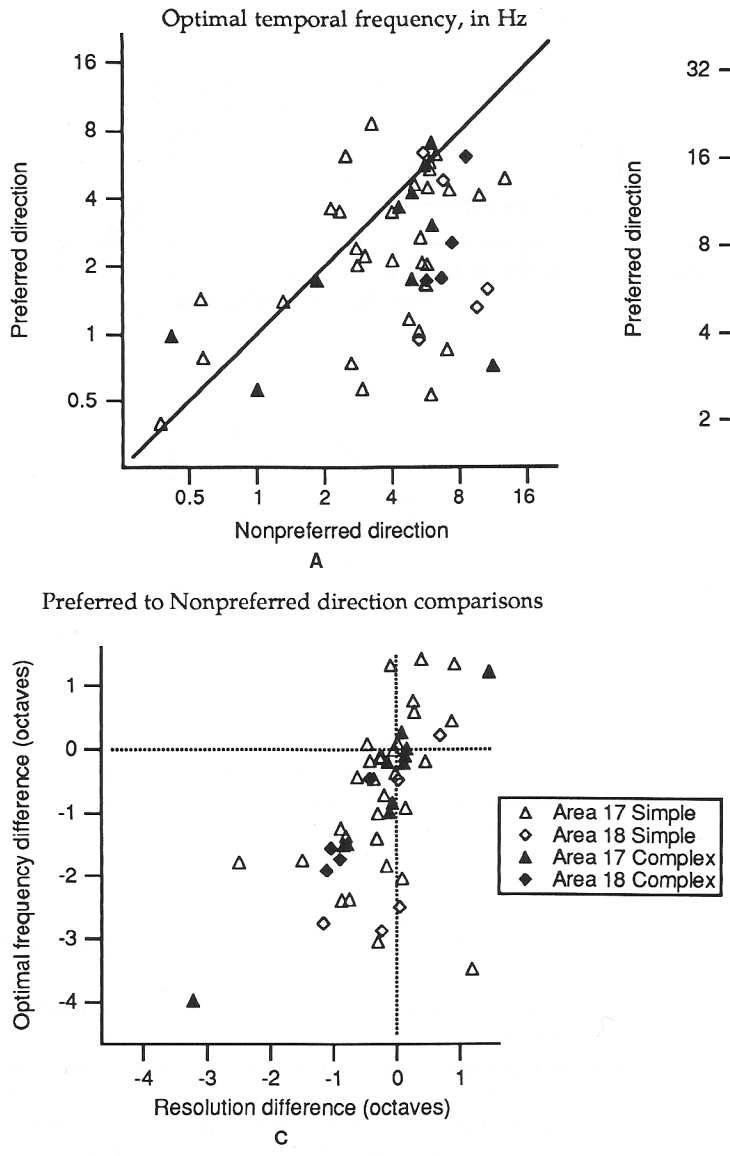

Fig. 4. Comparisons of temporal-frequency tuning between opposite directions of motion. A: Optimal temporal frequency in the preferred direction is plotted against optimal temporal frequency in the nonpreferred direction. 51 cells are included. The diagonal line runs through equal values in each direction, so that points below the line have lower preferred frequencies in the preferred direction. The filled symbols in this and the following graphs represent results from complex cells. Triangles and diamonds represent data from area 17 and area 18 neurons, respectively. B: Similar to A, but for temporal resolution. These 50 points (one cell had an undetermined resolution in the nonpreferred direction) show the high-frequency cutoff at 10% of the peak response, in each direction. C: For each cell, the difference in octaves between the two directions is plotted for the two parameters graphed in A and B. These 50 points show the distance of each cell from the diagonal lines in A and B. This plot illustrates the tendency for cells to have lower optimal frequencies in the preferred direction, without necessarily having lower resolutions.

of each point from the diagonal line is plotted. Points that fall below the horizontal line are those in Fig. 4A that fall below the diagonal line; points that lie to the left of the vertical line are those in Fig. 4B that fall below the diagonal line. This shows that cells with much lower optimal frequencies in the preferred direction can have similar resolutions in each direction. Whereas 40% of these cells had optimal frequencies at least an octave lower in the preferred direction, only 12% showed such a shift in resolution. The 12% with much lower resolution in the preferred direction were primarily cells that reversed their preferred direction, with the entire tuning curve roughly shifted along the temporal-frequency axis; these are the points toward the lower left corner of the plot. No cells had similar optimal frequencies but lower preferred direction resolutions (no points along the left-hand portion of the horizontal line). The preferred direction was on average tuned to 0.8 ± 0.2 octaves lower than the nonpreferred direction. The average difference in resolution was only 0.2 ± 0.1 octaves.

We estimated the range of temporal frequencies over which each cell was direction selective by taking the points where the *t*-score comparing the responses in the two directions exceeded a criterion value of 2. As an illustration, this criterion was easily achieved for the data in Figs. 1A and 1B at each temporal frequency below 4 Hz. It was also just met at 6 Hz and at 12 Hz in Fig. 1A, and at 8 Hz in Fig. 1B, with the preferred direction reversed. Most cells were direction selective at 1 and 2 Hz, and relatively few cells were direction selective at frequencies above 4 Hz. The percentage of cells that were direction selective ranged from 54% at 0.5 Hz, to 70% at 1 Hz and 78% at 2 Hz, down to 52% at 4 Hz, 28% at 8 Hz, and 12% at 16 Hz. There were also four cells in which the nonpreferred direction (at low frequencies) became preferred according to this criterion at frequencies above 2 Hz.

We repeated these experiments on nine lateral geniculate neurons, including four X_L (lagged-X), four X_N (nonlagged-X), and one Y_N (nonlagged-Y) cells. These cells contrasted markedly with the cortical cells. Whereas almost every cortical cell was direction selective at some temporal frequency, five of the nine geniculate cells showed no direction selectivity. Two others reached the criterion at a single temporal frequency, and two geniculate cells were slightly direction selective at three of ten temporal frequencies. The optimal temporal frequencies and

resolutions observed in the LGN were 3.4 Hz and 22 Hz, on average. In a larger sample of geniculate cells, we previously found mean optimal temporal frequencies of 3.1 ± 0.9 Hz for X_L cells, 4.7 ± 0.8 Hz for X_N cells, 4.7 ± 1.1 Hz for Y_L cells, and 6.0 ± 0.7 Hz for Y_N cells. Temporal resolutions were 17 ± 4 Hz for X_L cells, 25 ± 4 Hz for X_N cells, 18 ± 3 Hz for Y_L cells, and 26 ± 5 Hz for Y_N cells (Saul & Humphrey, 1990*a*). Thus, cortical temporal tuning (preferred direction optimal frequency of 3 Hz and resolution of 14 Hz) is similar to that of geniculate lagged cells.

Discussion

Our main result is that direction selectivity is strongest at low temporal frequencies, since the response in the nonpreferred direction tends to increase at high temporal frequencies. Often, direction selectivity is lost because of this increase, both directions responding equally at frequencies above about 4 Hz. In some cells, the preferred direction actually reverses. One consequence of these phenomena is a difference in optimal frequency between the two directions, with the preferred direction tuned to lower frequencies.

Holub and Morton-Gibson (1981) reported that 70% of cortical cells that gave significant responses in both directions differed in their spatial and/or temporal tuning. They found an average difference of 0.59 octaves in optimal temporal frequencies. They did not relate these differences to the preferred direction. We found that 40% of the cells that responded in both directions had optimal frequencies at least an octave lower in the preferred direction, and, averaged over the whole sample, the preferred direction was tuned to frequencies nearly an octave lower than the nonpreferred direction.

Reid (1988) also showed declining direction selectivity with temporal frequency, but did not specify any reasons for this decline other than a concomitant decline in receptive-field inseparability. We have confirmed that cortical receptive fields that are inseparable at 1 Hz often become more separable by 4 Hz, and that this correlates with a decline in direction selectivity (Saul & Humphrey, 1990*b*). Several studies have shown a correlation between spatiotemporal receptive-field structure and direction selectivity (Movshon et al., 1978; Reid et al., 1987, 1991; McLean & Palmer, 1989; Saul & Humphrey, 1990*b*; Tolhurst & Dean, 1991). Changes in response timing across simple cell receptive fields reliably predict preferred directions, and less reliably predict the degree of direction selectivity. This has led to some argument about the extent to which direction selectivity arises from linear *vs.* nonlinear mechanisms. A more important distinction (see, e.g. Reid et al., 1991) is whether direction selectivity arises from inputs that are not themselves direction selective (e.g. geniculate inputs), or from other directionally biased inputs (e.g. inhibition that is stronger in the nonpreferred direction). Multiple mechanisms may underlie the many occurrences of direction selectivity in visual cortex. In this study, we observed many cells that were direction selective at all temporal frequencies, including cells that maintained their selectivity up to high frequencies. However, a subset of our cells showed direction selectivity only at low temporal frequencies. For at least these cells, the range of acceptable models is restricted.

We suggest a tentative explanation for the cortical phenomenon described above based on our previous geniculate recordings (Saul & Humphrey, 1990*a*). The temporal-frequency tuning of direction selectivity could arise from interactions in cortex between lagged and nonlagged afferents. The signals from the geniculate afferents would be relayed through cortical neurons, and would comprise both excitatory and inhibitory influences. At low frequencies, these afferents respond approximately in temporal quadrature, and would therefore be expected to confer direction selectivity where they converged. By about 4 Hz, this quadrature relation is often lost, and direction selectivity would disappear. In this model, the temporal-frequency tuning of direction selectivity would depend more on timing relationships among the afferents than on their tuning. An alternative model might hold that inhibition is strongest in the nonpreferred direction, and is tuned so that at higher frequencies the inhibition becomes ineffective in blocking the nonpreferred direction response. This model would predict that reducing the inhibition by adapting in a cell's nonpreferred direction should improve the response to that direction, a phenomenon that is never observed (Saul & Cynader, 1989). Instead, the adaptation experiments indicate that direction-selective cells receive excitatory and inhibitory inputs that are not direction selective. Inhibition, in this view, is not direction selective but instead has particular timing relationships with the excitation. In the nonpreferred direction, the inhibition coincides with the excitation, whereas in the preferred direction the inhibition occurs out of phase with the excitation and hence is less effective.

In this sketch of a model, nothing is assumed about how the lagged and nonlagged inputs are combined. Although a simulation of this model (Saul & Humphrey, 1990*a*) was completely linear, this was only for simplicity. Even such a simple linear model captures much of the temporal-frequency tuning of direction selectivity. However, lagged and nonlagged inputs could be combined in many ways (multiplicative operations; *via* shunting inhibitory pathways; taking into account rectification) to obtain the same behavior. The key to this behavior is the relative response phase of the afferents. We note that complex cells also show the loss of direction selectivity at high temporal frequencies. These cells may be less likely to combine their inputs linearly than simple cells, since they show clear nonlinearities of spatial summation. However, ON- and OFF-center lagged and nonlagged inputs could converge (again, relayed through other cortical cells) onto single complex cells to produce the sort of direction-selective responses observed. Response rectification is a necessary component of the model described here in order to be realistic, since the geniculate inputs themselves are highly rectified. Such nonlinearities, which could help account for the tendency of a strictly linear model to overestimate the nonpreferred direction response amplitude (Reid et al., 1987, 1991; McLean & Palmer, 1989; Saul & Humphrey, 1990*b*; Tolhurst & Dean, 1991), do not imply a nonlinear suppression that is specific for the nonpreferred direction.

Consistent with the model of convergent lagged and nonlagged inputs, temporal resolution differs little between the two directions, despite the difference in optimal frequencies. As has been previously noted (Orban et al., 1985), cortical temporal resolution is much lower than that found in geniculate neurons. However, previous studies only took into account nonlagged LGN cells. Lagged X and Y cells have resolutions similar to those found in the cortex. The model of convergent lagged and nonlagged inputs predicts that cortical cells should have resolutions similar to their *excitatory* afferents, however. Our sample of geniculate neurons indicates that about 62% of the afferents in the central 10 deg have temporal resolution above 20 Hz, whereas only about 14% of our cortical cells had resolutions this high. Potential explanations for this discrepancy include the increasing potency of cortical adaptation at higher

temporal frequencies (Maddess et al., 1988; Saul & Cynader, 1989; Nelson, 1991; Bonds, 1991), susceptibility of cortical responses to anesthesia, other filtering properties of intracortical processing, and a more important role than expected for excitatory afferents from the lagged geniculate population.

Finally, we note that cortical direction selectivity is most profound at temporal frequencies of about 1–2 Hz. At these low frequencies, excitatory inputs must originate several hundred milliseconds after the inhibitory inputs that block them in the null direction. We have observed these long delays in the geniculate inputs (Saul & Humphrey, 1990*a*; cf. also Goodwin et al., 1975). These delays could be generated *de novo* in cortex, independent of the geniculate afferents. Our experiments are not capable of distinguishing between these possibilities. However, given that 40% of the X inputs to the cortex are lagged (Mastronarde, 1987; Humphrey & Weller, 1988*b*), it is reasonable to suggest that these geniculate inputs play a critical role in generating cortical direction selectivity at low temporal frequencies.

Acknowledgment

Chris Lucci and Paul Baker provided technical assistance in computer programming. We thank Jonathan Levitt for critical reading of the manuscript. This research was supported by Grants EY06034 and MH18273 to A.B. Saul, EY06459 to A.L. Humphrey, and a Core Grant For Vision Research (EY08098) to the Eye and Ear Institute of Pittsburgh.

References

Adelson, E.H. & Bergen, J.R. (1985). Spatiotemporal energy models for the perception of motion. *Journal of the Optical Society of America* **2**, 284–299.

Baker, C.L., Jr. & Cynader, M.S. (1986). Spatial receptive-field properties of direction-selective neurons in cat striate cortex. *Journal of Neurophysiology* **55**, 1136–1152.

Barlow, H.B. & Levick, W.R. (1965). The mechanism of directionally selective units in rabbit's retina. *Journal of Physiology* **178**, 477–504.

Bonds, A.B. (1991). Temporal dynamics of contrast gain in single cells of the cat striate cortex. *Visual Neuroscience* **6**, 239–255.

De Valois, R.L., Albrecht, D.G. & Thorell, L.G. (1982). Spatial-frequency selectivity of cells in macaque visual cortex. *Vision Research* **22**, 545–559.

Duysens, J., Maes, H. & Orban, G.A. (1987). The velocity dependence of direction selectivity of visual cortical neurones in the cat. *Journal of Physiology* **387**, 95–113.

Emerson, R.C. & Gerstein, G.L. (1977). Simple striate neurons in the cat. II. Mechanisms underlying directional asymmetry and directional selectivity. *Journal of Neurophysiology* **40**, 136–155.

Eysel, U.T., Wörgötter, F. & Pape, H.-C. (1987). Local cortical lesions abolish lateral inhibition at direction-selective cells in cat visual cortex. *Experimental Brain Research* **68**, 606–612.

Eysel, U.T., Muche, T. & Wörgötter, F. (1988). Lateral interactions at direction-selective striate neurones in the cat demonstrated by local cortical inactivation. *Journal of Physiology* **399**, 657–675.

Goodwin, A.W., Henry, G.H. & Bishop, P.O. (1975). Direction selectivity of simple striate cells: properties and mechanism. *Journal of Neurophysiology* **38**, 1500–1523.

Goodwin, A.W. & Henry, G.H. (1978). The influence of stimulus velocity on the responses of single neurons in the striate cortex. *Journal of Physiology* **277**, 467–482.

Holub, R.A. & Morton-Gibson, M. (1981). Response of visual cortical neurons of the cat to moving sinusoidal gratings: response-contrast functions and spatiotemporal interactions. *Journal of Neurophysiology* **46**, 1244–1259.

Humphrey, A.L., Sur, M., Uhlrich, D.J. & Sherman, S.M. (1985). Projection patterns of individual X- and Y-cell axons from the lateral geniculate nucleus to cortical area 17 in the cat. *Journal of Comparative Neurology* **233**, 159–189.

Humphrey, A.L. & Weller, R.E. (1988*a*). Functionally distinct groups of X-cells in the lateral geniculate nucleus of the cat. *Journal of Comparative Neurology* **268**, 429–447.

Humphrey, A.L. & Weller, R.E. (1988*b*). Structural correlates of functionally distinct X-cells in the lateral geniculate nucleus of the cat. *Journal of Comparative Neurology* **268**, 448–468.

Maddess, T., McCourt, M.E., Blakeslee, B. & Cunningham, R.B. (1988). Factors governing the adaptation of cells in area 17 of the cat visual cortex. *Biological Cybernetics* **59**, 229–236.

Mastronarde, D.N. (1987). Two classes of single-input X-cells in cat lateral geniculate nucleus. I. Receptive-field properties and classification of cells. *Journal of Neurophysiology* **57**, 357–380.

Mastronarde, D.N., Saul, A.B. & Humphrey, A.L. (1991). Lagged Y cells in the cat lateral geniculate nucleus. *Visual Neuroscience* **7**, 191–200.

McLean, J. & Palmer, L. (1989). Contribution of linear spatiotemporal receptive-field structure to velocity selectivity of simple cells in area 17 of cat. *Vision Research* **29**, 675–679.

Movshon, J.A., Thompson, I.D. & Tolhurst, D.J. (1978). Spatial summation in the receptive fields of simple cell in the cat's striate cortex. *Journal of Physiology* **283**, 53–77.

Mullikin, W.H., Jones, J.P. & Palmer, L.A. (1984). Receptive-field properties and laminar distribution of X-like and Y-like simple cells in cat area 17. *Journal of Neurophysiology* **52**, 350–371.

Nelson, S.B. (1991). Temporal interactions in the cat visual system. I. Orientation-selective suppression in the visual cortex. *Journal of Neuroscience* **11**, 344–356.

Orban, G.A., Kennedy, H. & Maes, H. (1981). Response to movement of neurons in areas 17 and 18 of the cat: direction selectivity. *Journal of Neurophysiology* **45**, 1059–1073.

Orban, G.A., Hoffman, K.-P. & Duysens, J. (1985). Velocity selectivity in the cat visual system. I. Responses of LGN cells to moving bar stimuli: a comparison with cortical areas 17 and 18. *Journal of Neurophysiology* **54**, 1026–1049.

Press, W.H., Flannery, B.P., Teukolsky, S.A. & Vetterling, W.T. (1986). *Numerical Recipes: The Art of Scientific Computing*. Cambridge, UK: Cambridge University Press.

Reid, R.C. (1988). *Directional selectivity and the spatiotemporal structure of the receptive fields of simple cells in cat striate cortex.* Ph.D. Dissertation, Rockefeller University.

Reid, R.C., Soodak, R.E. & Shapley, R.M. (1987). Linear mechanisms of directional selectivity in simple cells of cat striate cortex. *Proceedings of the National Academy of Sciences of the U.S.A.* **84**, 8740–8744.

Reid, R.C., Soodak, R.E. & Shapley, R.M. (1991). Directional selectivity and spatiotemporal structure of receptive fields of simple cells in cat striate cortex. *Journal of Neurophysiology* **66**, 505–529.

Saul, A.B. & Cynader, M.S. (1989). Adaptation in single units in visual cortex: the tuning of aftereffects in the temporal domain. *Visual Neuroscience* **2**, 609–620.

Saul, A.B. & Humphrey, A.L. (1989). Phase differences in the cat LGN and cortical direction selectivity. *Society for Neuroscience Abstracts* **15**, 1394.

Saul, A.B. & Humphrey, A.L. (1990*a*). Spatial and temporal response properties of lagged and nonlagged cells in cat lateral geniculate nucleus. *Journal of Neurophysiology* **64**, 206–224.

Saul, A.B. & Humphrey, A.L. (1990*b*). Evidence of lagged-type geniculate input to visual cortex. *Society for Neuroscience Abstracts* **16**, 1218.

Saul, A.B. & Humphrey, A.L. (1991). Cortical direction selectivity as a function of temporal frequency. *Society for Neuroscience Abstracts* **17**, 1015.

Shadlen, M. & Carney, T. (1986). Mechanisms of human motion perception revealed by a new cyclopean illusion. *Science* **232**, 95–97.

Tolhurst, D.J. & Doan, A.F. (1991). Evaluation of a linear model of directional selectivity in simple cells of the cat's striate cortex. *Visual Neuroscience* **6**, 421–428.

Van Santen, J.P.H. & Sperling, G. (1985). Elaborated Reichardt detectors. *Journal of the Optical Society of America* **2**, 300–321.

Watson, A.B. & Ahumada, A.J., Jr. (1983). A look at motion in the frequency domain. In *Motion: Perception and Representation*, ed. Tsotsos, J.K., pp. 1–10. New York: Association for Computing Machinery.

Watson, A.B. & Ahumada, A.J., Jr. (1985). Model of human visual-motion sensing. *Journal of the Optical Society of America* **2**, 322–342.